Journal of Medicinal Chemistry

Brief Article

Cite This: J. Med. Chem. 2018, 61, 2104−2110

pubs.acs.org/jmc

Development of Potent Inhibitors of Receptor Tyrosine Kinases by Ligand-Based Drug Design and Target-Biased Phenotypic Screening

Samuel H. Myers,[†] Carolin Temps,[†] Douglas R. Houston,[§] Valerie G. Brunton,[†] and Asier Unciti-Broceta*[,†]

[†]Cancer Research UK Edinburgh Centre, MRC Institute of Genetics and Molecular Medicine, University of Edinburgh, Crewe Road South, Edinburgh EH4 2XR, U.K.

[§]Institute of Quantitative Biology, Biochemistry and Biotechnology, University of Edinburgh, Edinburgh EH9 3BF, U.K.

Supporting Information

ABSTRACT: Pyrazolopyrimidines with potent antiproliferative properties were developed by an adaptive strategy that applies ligand-based design and phenotypic screening iteratively and is informed by biochemical assays. To drive development toward specific oncopathways, compounds were tested against cancer cells that overexpress, or not, AXL kinase. Identified phenotypic hits were found to inhibit oncotargets AXL, RET, and FLT3. Subsequent optimization generated antiproliferative lead compounds with unique selectivity profiles, including selective AXL inhibitors and a highly potent inhibitor of FLT3.

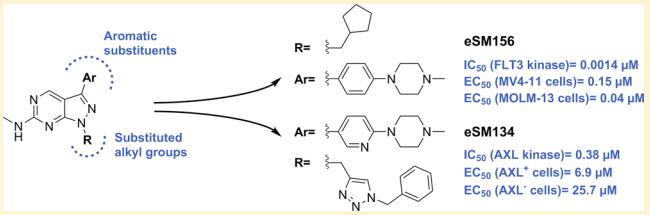

INTRODUCTION

The R&D costs of new drug development are continuously increasing, with figures of $1.4 billion being estimated as the average out-of-pocket cost to bring a new drug into the market.[1,2] In response to this challenging situation,[3] many medicinal chemistry laboratories are exploring strategies that prioritize the search for phenotypic hits over target-based approaches to accelerate the earlier stages of drug discovery.[4] Such strategies are particularly well suited to find multitargeted inhibitors against difficult-to-treat malignancies due to the heterogeneous nature of these cancers.[4−6] Using a strategy that combines ligand-based design of focused compound libraries and phenotypic screening in an iterative manner, our lab has recently reported the discovery of novel anticancer kinase inhibitors with suitable drug-like properties in a fraction of the time and preclinical R&D costs typically required in the industry.[7,8]

The transmembrane protein AXL is a receptor tyrosine kinase (RTK) that belongs to the TAM (TYRO3, AXL, and MER) subfamily. The oncogenic role of AXL has come under the spotlight in recent years due to its correlation with multiple cancer-promoting processes.[9] Incremented AXL signaling is associated with poor prognosis and drug resistance in both solid and hematological malignancies.[10] This oncogenic effect can be mediated through AXL overexpression, upregulation of its ligand GAS6, or by interaction with other RTKs (e.g., EFGR, HER2, FLT3),[9,11,12] highlighting the relevant and complex role of AXL in drug resistance to both targeted therapies and chemotherapy. While several FDA-approved kinase inhibitors have been found to inhibit AXL activity as a secondary target,[9] the absence of X-ray crystallographic data for the AXL kinase has limited the development of robust structure-based drug discovery activities until very recently (the first crystal structure of the AXL kinase domain in complex with an inhibitor was reported in 2017[13]).

Because of the timely need of making small molecules able to interfere with AXL oncogenic pathways, we embarked on a medchem campaign to search for phenotypically active kinase inhibitors. Inspired by published literature on inhibitors of MER (a TAM family member),[14] we investigated the development of focused libraries based on a pyrazolo[3,4-*d*]pyrimidine scaffold featuring an amino group at the C6 position (Figure 1). To drive development toward the discovery of kinase inhibitors that inhibit AXL signaling, cell viability assays were performed against two cancer cell lines: a drug resistant cancer cell line expressing AXL (positive discriminating cell model) and a cancer cell line that does not express AXL (negative discriminating cell model). After two rounds of synthesis and screening, followed by kinase inhibition profiling of selected hits showing preferential activity against the AXL-expressing cell line, novel phenotypically active inhibitors of AXL, RET, and FLT3 were discovered. Further optimization enabled the discovery of several lead compounds including eSM156, an FLT3 inhibitor with single-digit nM potency and high antiproliferative activity against acute myeloid leukemia (AML) cells.

RESULTS AND DISCUSSION

Design, Synthesis, and Screening of Compounds 7a−j. Wang and co-workers[14] explored the development of trisubstituted pyrazolopyrimidines as MER inhibitors based

Received: October 30, 2017
Published: February 21, 2018

DOI: 10.1021/acs.jmedchem.7b01605
J. Med. Chem. 2018, 61, 2104−2110

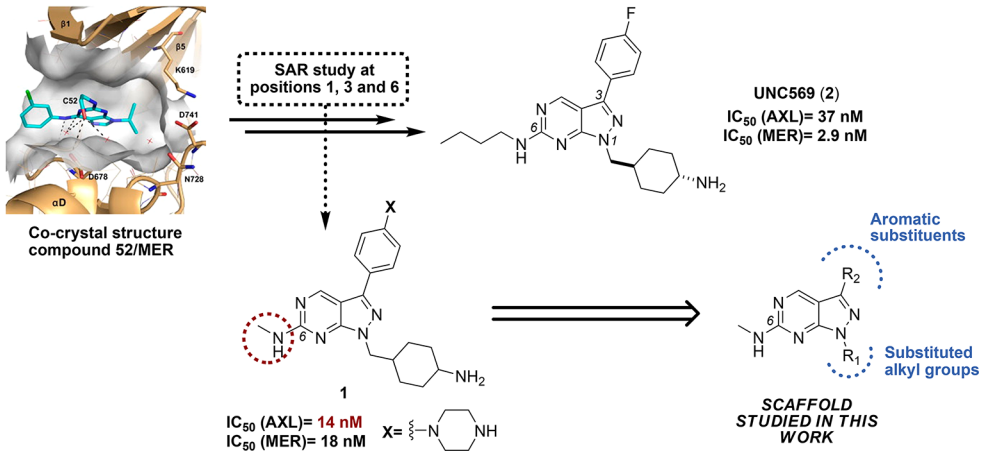

Figure 1. Medicinal chemistry campaign based on the cocrystal structure of **52** and MER (PDB 2G15[15]) performed by Wang and co-workers[13] for the discovery of MER inhibitor UNC569 and the 6-methylaminopyrazolo[3,4-*d*]pyrimidine scaffold explored in this work.

Scheme 1. Four-Step Synthetic Route for the Preparation of Compounds 7a–j from Commercially Available 6-Chloro-1*H*-pyrazolo[3,4-*d*]pyrimidine, 3

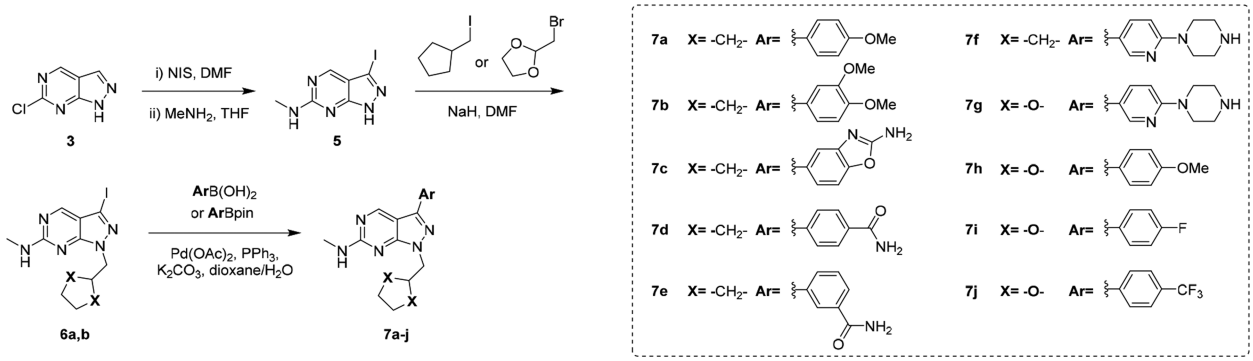

on a docking study with the cocrystal structure of MER and derivative **52**.[15] Because the TAM family kinases show remarkable similarities to one another, in addition to MER, all compounds were tested against AXL and TYRO3. Exploration at the C6 position with various alkylamino groups showed that the larger the alkyl, the higher the degree of selectivity for MER over AXL. Notably, the use of a methylamino group at that position resulted in a potent inhibitor exhibiting superior potency for AXL than for MER (**1**, Figure 1). This observation served as the starting point of the ligand-based design explored in this work.

A 10-member library of derivatives of **1** was synthesized using the synthetic route described in Scheme 1 (see full details in the Supporting Information). Commercially available 6-chloro-1*H*-pyrazolo[3,4-*d*]pyrimidine, **3**, was treated with *N*-iodosuccinimide to iodinate the C3 position of the heterocycle (94% yield) and thus generate an activated position for Suzuki–Miyaura cross-coupling. The chloro atom at the C6 position of **4** was then substituted via a S_NAr with methylamine in THF to give **5** in moderate yield (55%). On the basis of in-house investigations[7] suggesting that the presence of a methylene-linked saturated five-membered ring at the N1 position of pyrazolopyrimidine scaffolds enhances kinase inhibition activity, intermediate **5** was alkylated via reaction with iodomethylcyclopentane or 3-bromomethyl-1-3-dioxolane to give **6a,b** in moderate yield (41%). 3-Aryl derivatives **7a–j** were prepared via Suzuki coupling in moderate to good yields (29–72%).

Derivatives **7a–j** were then tested against two breast cancer cell lines: BT474 cells (AXL^-), which does not express AXL, and AXL-overexpressing mouse breast cancer cells (AXL^+), a cell line created in-house which is resistant to the pan-HER inhibitor sapatinib. AXL^+ and AXL^- cells were used as a positive and negative discriminating cell model, respectively, with the aim to find compounds with preferential activity against AXL^+ cells and thereby bias subsequent chemical design toward the inhibition of AXL-associated oncopathways, without ruling out that further proteomics differences between these cell lines could drive the design toward additional targets. Reduction of cell proliferation was employed as the primary screening output, using the pan-RTK inhibitor foretinib (which is reported to inhibit AXL at 11 nM)[9] as a positive control. EC_{50} values were calculated using 8-point half-log dose–response assays (0.03–100 μM) and the results plotted in Figure 2. The phenotypic screen showed that the majority of the compounds in this series were more active against AXL^+ cells than AXL^-, with three compounds, **7f**, **7g**, and **7h**, displaying EC_{50} values equal to or lower than 10 μM. The most potent compound from this series was **7f**, which exhibited sub-μM activity (0.83 μM) against AXL^+ cells and a 2-fold potency increase over the AXL^- BT474 cell line (1.64 μM). Notably, the antiproliferative potency of its close analogue **7g** (containing a dioxolane group instead of a cyclopentane) was an order of magnitude lower, indicating that the presence of one or more oxygen atoms in that moiety negatively affects activity. Because of the high potency of **7f** and its promising

DOI: 10.1021/acs.jmedchem.7b01605
J. Med. Chem. 2018, 61, 2104–2110

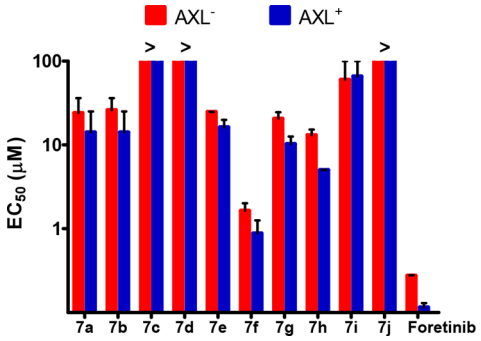

Figure 2. EC_{50} values of **7a–j** and the positive control foretinib against AXL^- (red) and AXL^+ (blue) cells. Cell viability assay: PrestoBlue reagent at day 5. Error bars: ±SD from $n = 2$.

$EC_{50}(AXL^-)/EC_{50}(AXL^+)$ ratio, the 6-(1-piperazinyl)-pyrid-3-yl group of **7f** was chosen as the C3 motif for the preparation of a second library of pyrazolopyrimidines.

Design, Synthesis, and Screening of Compounds 10a–g. The second library was designed to explore the incorporation of more complex moieties at the N1 position of the pyrazolopyrimidine. Because the presence of a methylene-linked five-membered ring at that position generated compounds with high activity and the 1,3-dioxolanylmethyl group was found to be suboptimal, other heteroaromatic rings were considered. To the best of our knowledge, the introduction of substituted triazolylmethyl groups at the N1 position of the scaffold studied in this work have not yet been reported. A substituted 1,2,3-triazole group (Scheme 2) was thus selected to facilitate the preparation of different analogues by click chemistry, study novel structure–activity relationships (SAR), and add freedom-to-operate to the chemical space under exploration. The alkyne handle was introduced by alkylation of intermediate **5** with propargyl bromide, giving *N*-propargyl derivative **8** in 23% yield. Copper-catalyzed azide–alkyne cycloadditions were carried out with seven different organic azides using copper iodide, sodium ascorbate, and triethylamine to give **9a–g** in good yields (>66%). Palladium-catalyzed Suzuki cross-coupling of the triazole-containing derivatives **9a–g** with 6-(1-piperazinyl)pyridyl-4-boronic acid pinacol ester provided final compounds **10a–g**.

Scheme 2. Synthetic Route for the Preparation of Triazole-Containing Compounds 10a–g from Intermediate 5

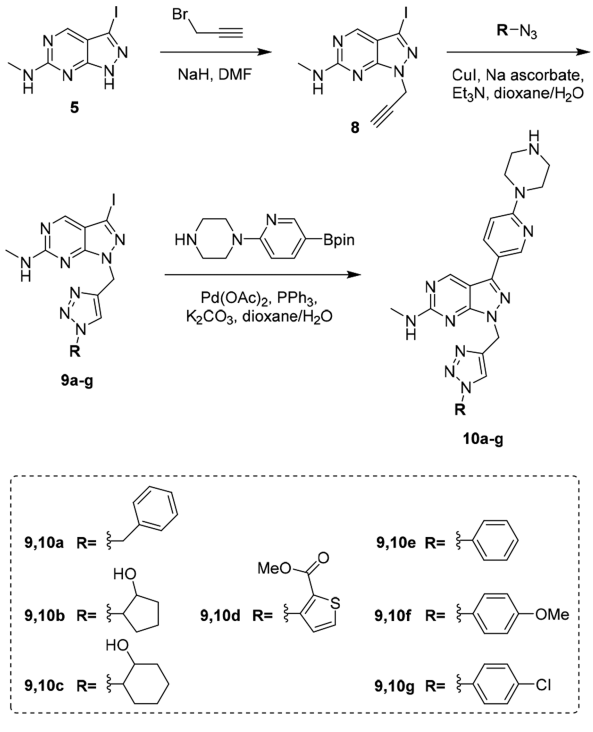

The antiproliferative activity of **10a–g** was then tested against AXL^- and AXL^+ cells. As shown in Figure 3, the most potent derivatives of this series were **10a** (R = benzyl) and **10d** (R = 2-(methoxycarbonyl)thienyl)), both of which exhibited superior antiproliferative activity against AXL^+ cells. However, the potency of **10a** and **10d** was lower than that of the phenotypic hit **7f**. The introduction of aliphatic rings (**10b,c**) at the 3′ position of the triazole ring led to a dramatic reduction in potency. The direct linkage of phenyl rings to the 3′ position of the triazole (**10e–g**) did not improve activity over the benzyl-containing derivative **10a**.

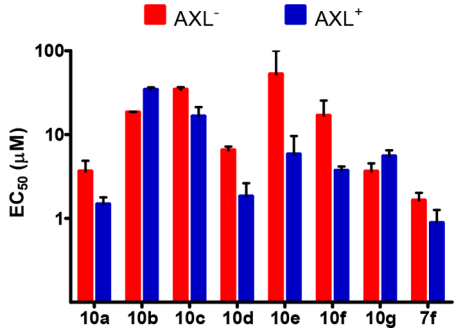

Figure 3. EC_{50} values of **10a–g** and reference hit **7f** against AXL^- (red) and AXL^+ (blue) cells. Cell viability assay: PrestoBlue reagent at day 5. Error bars: ±SD from $n = 2$.

To shed light over the pharmacodynamic profile responsible for the antiproliferative properties of phenotypic hits **7f,g,h** and **10a,d**, kinase inhibition activities were evaluated against a panel of 12 protein kinases. The panel, which included the three members of the TAM family, was selected based on the selectivity profile frequently found for other AXL inhibitors.[9] Kinase inhibition studies were performed by Reaction Biology Corporation, USA, by measuring ^{33}P incorporation on the corresponding kinase substrate relative to DMSO. Calculated half-maximal inhibitory concentration (IC_{50}) values are shown in Table 1.

The results from the kinase screenings confirmed that the most potent phenotypic hits from both libraries inhibited AXL kinase activity at low μM to sub-μM levels. However, much like many reported AXL inhibitors,[9] in most cases the primary target was not the AXL kinase, with FLT3 and RET being the most potently inhibited kinases across the screen. Of note, all the hits showed selectivity over the TAM family members TYRO3 and MER, proving the importance of using a methylamino group at the C6 position of the scaffold to achieve subfamily selectivity. In agreement with the cell-based assays, derivative **7f** displayed the greatest activity against AXL, FLT3, and RET: 0.12, 0.02, and 0.05 μM, respectively. Arguably, the most interesting hit from this screening was the 3′-benzyltriazolyl derivative **10a**, which exhibited the second highest potency against AXL (0.4 μM) and, importantly, was the only inhibitor to display superior activity for AXL than for

DOI: 10.1021/acs.jmedchem.7b01605
J. Med. Chem. 2018, 61, 2104–2110

Table 1. IC_{50} Values (in μM) for 7f,g,h and 10a,d against a Selection of Recombinant Tyrosine Kinases

kinase/hit	7f	7g	7h	10a	10d
AKT	>10	>10	>10	>10	>10
Aurora A	0.16	0.66	0.56	1.8	0.79
AXL[a]	**0.12**	**0.53**	**1.3**	**0.40**	**0.78**
KIT	1.1	7.5	>10	>10	>10
MER[a]	0.64	6.2	8.7	2.3	8.9
MET	2.1	>10	>10	>10	>10
SRC	1.1	0.89	7.2	1.0	>10
FLT3	**0.02**	**0.10**	**0.25**	**0.53**	**0.86**
VEGFR2	0.69	4.5	7.5	>10	>10
mTOR	>10	>10	>10	>10	>10
RET	**0.05**	**0.16**	**1.2**	**0.60**	**0.43**
TYRO3[a]	>10	>10	>10	>10	>10

[a]Member of TAM subfamily.

FLT3 and RET. This preferential selectivity against AXL was not observed with the close derivative **10d**, suggesting that the flexible benzyl group provides a certain degree of conformational freedom that is advantageous for binding to the AXL protein but less favorable for FLT3 and RET.

Design, Synthesis, and Screening of Compounds 12a–f. On the basis of the cell assays and the kinase screening, six new derivatives of **10a** were prepared to search for improved AXL inhibition. **12a–f** were prepared in moderate yields (27–58%) by Suzuki cross-coupling of intermediate **9a** with six different arylboronate/boronic acids. The diversity of the moieties incorporated at the C3 position (Figure 4) aimed to evaluate the importance of the H-donor and acceptors of the 6-(1-piperazinyl)-pyrid-3-yl moiety of **10a**.

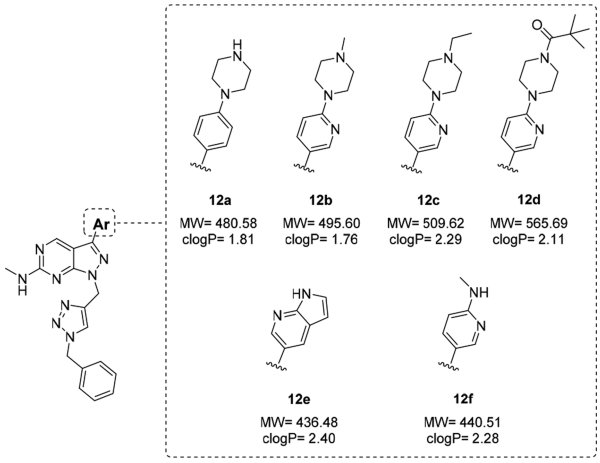

Figure 4. Structure, molecular weight (MW), and cLogP of derivatives **12a–f**.

Following the protocol described above, **12a–f** were tested against AXL^- and AXL^+ cells and the resulting EC_{50} values plotted in Figure 5. Whereas none of the new analogues improved the activity of **10a** against the AXL^+ cell line, **12b** showed a superior $EC_{50}(AXL^-)/EC_{50}(AXL^+)$ ratio, potentially indicating enhanced AXL selectivity. Interestingly, the seemly minor substitution of the pyridine N atom by a CH led to an inversion of the cell activity ratio, pointing out off-target effects. It was also noticeable that the attachment of large groups at the piperazinyl NH (**12c,d**) reduced antiproliferative activity against the AXL^+ cell line. The substitution of the pyperazinyl

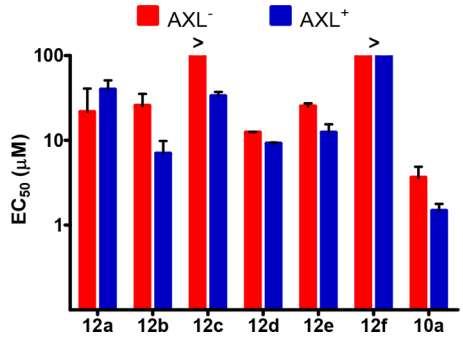

Figure 5. EC_{50} values of **12a–f** and reference hit **10a** against AXL^- (red) and AXL^+ (blue) cells. Cell viability assay: PrestoBlue reagent at day 5. Error bars: ±SD from $n = 2$.

group by methylamino (**12f**) resulted in a completely inactive derivative.

To understand how these structural changes had affected the kinase selectivity of the new compounds, **12a–d** were screened against the 12-member panel of kinases used for previous hits. As before, kinase inhibition screenings were performed using radioisotope based methods by Reaction Biology Corporation. Inhibitor BGB324, which is widely considered a selective AXL inhibitor (even if the available kinase selectivity information is limited)[9] and the first one to enter clinical trials based on its AXL inhibitory properties,[16] was used as a positive control. Calculated IC_{50} values are shown in Table 2.

Table 2. IC_{50} Values (in μM) for 12a–d and BGB324 against a Selection of Recombinant Tyrosine Kinases

kinase/hit	12a	12b	12c	12d	BGB324
AKT	>10	>10	1.9	>10	>10
Aurora A	>10	0.73	>10	0.84	0.026
AXL[a]	**>10**	**0.38**	**>10**	**0.76**	**0.0007**
KIT	>10	>10	>10	>10	1.0
MER[a]	>10	2.0	>10	5.4	0.015
MET	>10	>10	6.3	>10	3.4
SRC	>10	8.3	>10	>10	0.037
FLT3	**>10**	**0.70**	**>10**	**1.2**	**0.0009**
VEGFR2	>10	7.6	7.7	>10	0.008
mTOR	>10	>10	>10	>10	>10
RET	**>10**	**0.90**	**6.2**	**4.0**	**0.003**
TYRO3[a]	>10	>10	1.9	>10	0.017

[a]Member of TAM subfamily.

As shown in Table 2, derivative **12b** exhibited superior AXL inhibition (0.38 μM) and an increased degree of selectivity over FLT3 and RET in comparison to reference hit **10a**. In silico studies provided preliminary insights into the binding mode of 12b in AXL and RET (see the Supporting Information). It is important to note that **10a** displayed higher antiproliferative activity against AXL^+ cells (Figure 5), which may be caused by superior cell permeant properties or by unidentified off-target activities. The rest of the compounds of this series were not as potent as **12b** and showed poorer selectivity profiles. Derivative **12a**, which was previously found to display a $EC_{50}(AXL^-)/EC_{50}(AXL^+) < 1$, did not elicit inhibition to any of the kinases tested in the screen, further proof that its "inversed" antiproliferative properties are a consequence of targeting proteins unrelated to AXL-associated oncopathways. Remarkably, the screening revealed that the supposedly AXL-selective

DOI: 10.1021/acs.jmedchem.7b01605
J. Med. Chem. 2018, 61, 2104–2110

inhibitor BGB324 actually inhibits both AXL and FLT3 kinases with equivalent potency. This information, which to our knowledge is reported herein for the first time, further illustrates the difficulty of designing selective AXL inhibitors due to the structural similarities of the catalytic domains of AXL and other RTKs (e.g., FLT3 and RET). Furthermore, it underlines the value of discovering cell-active AXL kinase-selective inhibitors such as **10a** and **12b**.

Design, Synthesis, and Screening of Compounds 13a−d. At this point of the campaign, only **7f** exhibited sub-μM antiproliferative activity against the AXL$^+$ breast cancer cell model. According to the kinase screen (Table 1), **7f** inhibited AXL with high potency (0.12 μM) and displayed even higher potency against FLT3 and RET (0.02 and 0.05 μM, respectively). These two RTKs have been strongly linked to various malignancies. FLT3 is upregulated in acute lymphoblastic leukemia,[17] and the *FLT3-ITD* mutation is found in 30−40% of adult AML patients and associated with low survival rates. Because of its prognostic importance, the WHO recommends ascertaining the mutational status of *FLT3* in AML patients.[18] RET has been linked to numerous cancer types, including pancreatic,[19] breast cancer,[20] and AML.[21] RET is associated with metastasis and cancer relapse, being a predictor of acquired resistance and poor patient prognosis. Because AXL has also been associated with AML,[22] following the lab's ethos of evolving development in response to inhibitors' properties to accelerate the discovery of lead compounds,[8] the program was steered toward AML.

Four derivatives featuring a cyclopentylmethyl moiety at N1 position (as **7f**) were prepared by Suzuki coupling of intermediate **6a** with the corresponding arylboronate/boronic acids. The substituents at the C3 position of **13b−d** (Figure 6)

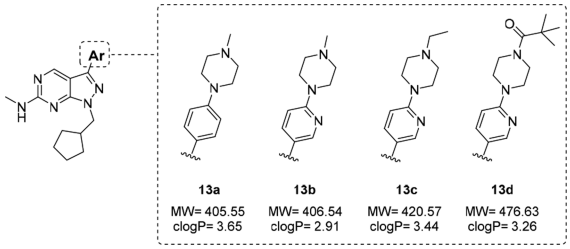

Figure 6. Structure, MW, and cLogP of derivatives **13a−d**.

were the same as the ones previously used for **12b−d** (Figure 4). However, because derivative **12a** displayed no inhibition of AXL, FLT3, or RET (see Table 2), a *N*-methyl derivative of the 4-pyperazinylphenyl group used in **12a** was incorporated at C3 on derivative **13a**.

The antiproliferative properties of **13a−d** were tested against the AML cell lines MV4-11 (homozygous *FLT3/ITD* mutant[25]) and MOLM-13 (heterozygous for *FLT3/ITD* mutation[25]), using the dual AXL/FLT3 inhibitor BGB324 as a positive control. As shown in Figure 7, derivatives **13a** and **13b** displayed sub-μM EC_{50} values, highlighting the potent antiproliferative activity of derivative **13a**, which displayed in both cell lines superior potency than BGB324, an inhibitor that is currently in clinical development for the treatment of AML.[23]

Given the fairly similar MW and cLogP of derivatives **13a−d** (Figure 6), it was anticipated that the different antiproliferative activity observed for each member of this series were caused by variations in on-target potency. Biochemical assays were then performed for **13a−d** against the 12 recombinant kinases tested

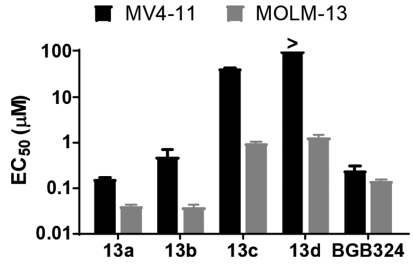

Figure 7. EC_{50} values of **13a−d** and BGB324 against MV4-11 and MOLM-13 cells. Cell viability assay: PrestoBlue reagent at day 5. Error bars: ±SD from n = 2.

before. As shown in Table 3, the analogues' activity against FLT3 correlated with their antiproliferative activity in AML

Table 3. IC_{50} Values (in μM) for 13a−d and BGB324 against a Selection of Recombinant Kinases

kinase/hit	13a	13b	13c	13d	BGB324
AKT	>10	>10	>10	>10	>10
ALK	0.05	0.19	ND	ND	0.53
Aurora A	0.006	0.03	0.28	0.61	0.026
Aurora B	0.1	0.17	ND	ND	0.1
AXL[a]	**0.013**	**0.07**	**0.26**	**7.2**	**0.0007**
DDR1	0.035	0.1	ND	ND	0.02
EFGR	>10	>10	ND	ND	3.9
KIT	0.068	0.36	1.8	>10	1.0
MER[a]	0.092	0.48	2.5	>10	0.015
MET	0.42	3.5	>10	>10	3.4
SRC	0.093	0.8	3.6	>10	0.037
FLT3	**0.0014**	**0.008**	**0.1**	**0.3**	**0.0009**
FLT3 ITD	**0.011**	**0.03**	ND	ND	**0.006**
FLT3 D835Y	**0.004**	**0.012**	ND	ND	**0.002**
PDGFRa	0.37	0.99	ND	ND	0.02
VEGFR2	0.066	0.40	1.9	>10	0.008
mTOR	>10	>10	>10	>10	>10
RET	**0.006**	**0.06**	**0.44**	**>10**	**0.003**
TYRO3[a]	0.6	3.67	>10	>10	0.017

[a]Member of TAM subfamily. ND: not determined.

cells. Derivative **13a**, the most potent inhibitor of the series, displayed 1.4 nM activity (IC_{50}) against FLT3 and IC_{50} values ranging from 6 to 13 nM for Aurora A, RET, and AXL. To attain a more detailed picture of the selectivity of the best hits, **13a,b** and BGB324 were further screened against a selection of eight kinases commonly inhibited by FLT3 inhibitors: ALK, Aurora B, DDR1, EGFR, PDGFRa, and FLT3 mutants FLT ITD and FLT3 835Y. Derivative **13a** showed selectivity over EGFR and PDGFRa, exhibited moderate potency against Aurora B and DDR1, and high potency against ALK, FLT ITD, and FLT3 835Y. The same trend was observed for **13b**, although displaying a potency reduction of 4−8-fold relative to **13a**. In comparison with the clinical candidate BGB324, the potent inhibitor **13a** displayed 2-fold lower potency against RET, FLT3, and its mutants and 4-fold superior potency against Aurora A. However, it exhibited a 20-fold reduction in activity against AXL. It is important to note that **13a** showed superior potency against MV4-11 and MOLM-13 cells, which may be due to improved membrane permeant properties or to the inhibition of other targets such as Aurora A.

Because of the high potency of **13a** in vitro and in cells, an expanded kinome inhibition study was performed (single dose

DOI: 10.1021/acs.jmedchem.7b01605
J. Med. Chem. 2018, 61, 2104−2110

of 1 μM, in duplicate) against 369 wild-type kinases. Enzymatic inhibition was compared to DMSO (= 0% inhibition) and averaged results plotted in a kinome phylogenetic tree with a 65% cutoff value using TREEspot from DiscoveRx (Figure 8;

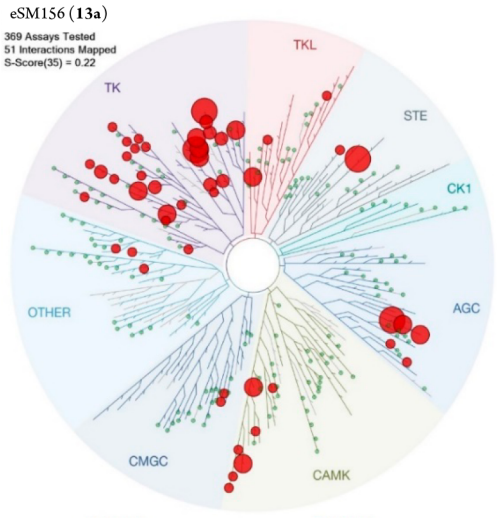

Figure 8. Map of the human kinome screened for **13a** at 1 μM. Green circles denote <65% inhibition. Red circles denote >65% inhibition (>98% for the largest one).

values listed in Supporting Information, Table 1). The study gave a *S*-score of 0.22 and, although not as potent as FLT3, most hits (>65% inhibition) belonged to the tyrosine kinase family. Besides FLT3, the tyrosine kinase JAK3 was also inhibited at levels superior to 98%. This is relevant as *JAK3* is a proto-oncogene associated with different leukemias.[24] Other strongly inhibited proteins from different families included ARK5, MAP4K family kinases, LRRK2, MINK1, RSK4, TNIK, TRKC, and TYK2.

CONCLUSIONS

Using an adaptive approach that combines ligand-based design of small libraries of pyrazolopyrimidines, target-informative cancer cell assays, and kinase screenings, two selective AXL inhibitors and a potent FLT3 inhibitor have been developed. The discovery of cell active AXL inhibitors **10a** (eSM119) and **12b** (eSM134) is relevant due to the lack of inhibitors that targets AXL with selectivity over TAM family members MER and TYRO3 and other RTKs (e.g., RET, FLT3). The merit of developing these lead compounds is further highlighted by the finding that BGB324, the only inhibitor in clinical development presumed to be selective for AXL,[16] is actually a dual AXL/FLT3 inhibitor. By steering the program toward AML, the potent FLT3 inhibitor **13a** (eSM156) was discovered, which displays single-digit nM IC_{50} against FLT3 and its mutants and low sub-μM EC_{50} against AML cells. Given its remarkable biological properties, eSM156 represents an attractive lead for future optimization against FLT3 and other proteins discovered in the kinome screening.

EXPERIMENTAL SECTION

General. Chemicals were purchased from Fisher, Sigma-Aldrich, or VWR. Microwave reactions were carried out in a Biotage Initiator. NMR spectra were recorded at rt on a 500 MHz Bruker Avance III spectrometer. Chemical shifts are reported in ppm relative to solvent peak. Analytical TLC was performed on Merck TLC Silica Gel 60 F254 plates and visualized by UV light. Purifications were performed by flash chromatography with commercially available silica gel and solvents. All compounds used in the biological screenings were determined to be >95% pure by HPLC.

Synthesis of 3-Iodo-*N*-methyl-1*H*-pyrazolo[3,4-*d*]pyrimidin-6-amine (5). *N*-Iodosuccinimide (1.9 g) was added to a suspension of 6-chloro-1*H*-pyrazolo[3,4-*d*]pyrimidine (1.0 g) in DMF (15 mL) and microwave-heated at 120 °C for 1 h. H_2O (50 mL) and EtOAc (50 mL × 3) were added, and the organic layers were collected, washed with H_2O (30 mL × 2) and brine (20 mL), dried over anhydrous $MgSO_4$, and concentrated in vacuo. Flash chromatography (MeOH/DCM 0−2%) yielded **4** as a yellow solid (1.64 g, 91%). ^{1}H NMR (500 MHz, DMSO) δ 14.64 (1 H, s, NH), 9.02 (1 H, s, CH). LRMS (+ve) *m*/*z* [M + 1] 281.00. **4** (500 mg) was dissolved in THF (3 mL), added to CH_3NH_2 (12 mL), and microwave heated at 150 °C for 1 h. A white solid precipitated out, dried by vacuum filtration, and washed with H_2O (3 mL × 3) to yield **5** as a beige solid (270 mg, 55%). ^{1}H NMR (500 MHz, DMSO) δ 12.61 (1 H, s), 8.46 (1 H, s), 7.54 (1 H, s), 2.83 (3 H, d, *J* = 3.5). ^{13}C NMR (126 MHz, DMSO) δ 162.7, 157.1, 153.9, 134.2, 93.3, 67.5, 28.5. HRMS (ESI +ve) *m*/*z* [M + 1] 275.9737.

Synthesis of 1-(Cyclopentylmethyl)-*N*-methyl-3-[4-(4-methylpiperazin-1-yl)phenyl]-1*H*-pyrazolo[3,4-*d*]pyrimidin-6-amine (13a). **5** (265 mg) in DMF (3 mL) was added NaH (34 mg) and stirred until gas evolution subsided. (Iodomethyl)cyclopentane (0.182 mL) was added dropwise and the resulting mix microwave-heated for 1.5 h at 150 °C. H_2O (50 mL) and EtOAc (50 mL × 3) were added, and the organic layers were collected, washed with water (30 mL × 2) and brine (20 mL), dried over anhydrous $MgSO_4$, and concentrated in vacuo. The crude was purified by flash chromatography MeOH/DCM (0−5%) to give **6a** as a yellow solid (133 mg, 40%). ^{1}H NMR (500 MHz, DMSO) δ 8.44 (1 H, s, NH), 7.61 (1 H, s), 4.11 (2 H, s), 2.86 (3 H, s), 1.65−1.21 (9 H, m). ^{13}C NMR (126 MHz, DMSO) δ 162.5, 155.8, 154.2, 112.0, 92.3, 50.7, 32.1, 30.1, 28.3, 24.8. HRMS (ESI +ve) *m*/*z* [M + 1] 358.0523. **6a** (60 mg), 4-(4-methylpiperazin-1-yl)phenylboronic acid (76 mg), K_2CO_3 (34 mg), PPh_3 (20%mol), and $Pd(OAc)_2$ (5%mol) were dissolved in 9:1 dioxane/water (5 mL) and microwave-heated at 120 °C for 1 h. H_2O (50 mL) and EtOAc (50 mL × 3) were added, and the organic layers were collected, washed with water (30 mL × 2) and brine (20 mL), dried over anhydrous $MgSO_4$, and concentrated in vacuo. The crude was purified by flash chromatography (MeOH/DCM 0−10%) to yield **13a** as a yellow solid (31 mg, 45%). ^{1}H NMR (500 MHz, $CDCl_3$) δ 8.93 (1 H, s), 7.83 (2 H, m), 7.04 (2 H, m), 4.25 (2 H, d, *J* = 7.5,), 3.34 (5 H, m), 3.09 (3 H, d, *J* = 5.0), 2.65 (6 H, d, *J* = 6.0), 2.41 (4 H, s), 1.41 (2 H, d, *J* = 5.5), 1.28 (3 H, s). ^{13}C NMR (126 MHz, $CDCl_3$) δ 161.4, 156.0, 153.5, 151.3, 143.9, 127.8, 115.9, 54.9, 50.8, 48.5, 46.1, 40.2, 30.3, 28.6, 24.9. HRMS (ESI +ve) *m*/*z* [M + 1] 406.2132.

ASSOCIATED CONTENT

Supporting Information

The Supporting Information is available free of charge on the ACS Publications website at DOI: 10.1021/acs.jmedchem.7b01605.

Characterization of compounds, docking studies, and biological methods (PDF)

Molecular formula strings (CSV)

AUTHOR INFORMATION

Corresponding Author

*Phone: (44)1317773584. Fax: (44)1317773520. E-mail: Asier.Unciti-Broceta@igmm.ed.ac.uk.

ORCID

Asier Unciti-Broceta: 0000-0003-1029-2855

Author Contributions

All authors approved the final version of the manuscript.

DOI: 10.1021/acs.jmedchem.7b01605
J. Med. Chem. 2018, 61, 2104−2110

Notes

The authors declare no competing financial interest.

■ ACKNOWLEDGMENTS

We thank Scottish Power and CRUK for funding. C.T. thanks the CMVM for a Principal's Scholarship.

■ ABBREVIATIONS USED

AML, acute myeloid leukemia; IC_{50}, half-maximal inhibitory concentration; RTK, receptor tyrosine kinase; S_NAr, nucleophilic aromatic substitution; TAM, TYRO3, AXL and MER

■ REFERENCES

(1) Avorn, J. The $2.6 Billion pill — methodologic and policy considerations. *N. Engl. J. Med.* **2015**, *372*, 1877−1879.
(2) DiMasi, J. A.; Grabowski, H. G.; Hansen, R. W. Innovation in the pharmaceutical industry: New estimates of R&D costs. *J. Health. Econ.* **2016**, *47*, 20−33.
(3) Kola, I.; Landis, J. Can the pharmaceutical industry reduce attrition rates? *Nat. Rev. Drug Discovery* **2004**, *3*, 711−716.
(4) Lee, J. A.; Uhlik, M. T.; Moxham, C. M.; Tomandl, D.; Sall, D. J. Modern phenotypic drug discovery is a viable, neoclassic pharma strategy. *J. Med. Chem.* **2012**, *55*, 4527−4538.
(5) Knight, Z.; Lin, H.; Shokat, K. M. Targeting the cancer kinome through polypharmacology. *Nat. Rev. Cancer* **2010**, *10*, 130−137.
(6) Carragher, N.; Unciti-Broceta, A.; Cameron, D. Advancing drug discovery towards more agile development of targeted combination therapies. *Future Med. Chem.* **2012**, *4*, 87−105.
(7) Fraser, C.; Carragher, N. O.; Unciti-Broceta, A. eCF309: a potent, selective and cell-permeable mTOR inhibitor. *MedChemComm* **2016**, *7*, 471−477.
(8) Fraser, C.; Dawson, J. C.; Dowling, R.; Houston, D. R.; Weiss, J. T.; Munro, A.; Muir, M.; Harrington, L.; Webster, S. P.; Frame, M.; Brunton, V.; Patton, E. E.; Carragher, N. O.; Unciti-Broceta, A. Rapid discovery and structure−activity relationships of pyrazolopyrimidines that potently suppress breast cancer cell growth via SRC kinase inhibition with exceptional selectivity over ABL kinase. *J. Med. Chem.* **2016**, *59*, 4697−4710.
(9) Myers, S. H.; Brunton, V. G.; Unciti-Broceta, A. AXL inhibitors in cancer: A medicinal chemistry perspective. *J. Med. Chem.* **2016**, *59*, 3593−3608.
(10) Gay, C. M.; Balaji, K.; Byers, L. A. Giving AXL the axe: targeting AXL in human malignancy. *Br. J. Cancer* **2017**, *116*, 415−423.
(11) Park, I. K.; Mundy-Bosse, B.; Whitman, S. P.; Zhang, X.; Warner, S. L.; Bearss, D. J.; Blum, W.; Marcucci, G.; Caligiuri, M. A. Receptor tyrosine kinase Axl is required for resistance of leukemic cells to FLT3-targeted therapy in acute myeloid leukemia. *Leukemia* **2015**, *29*, 2382−2389.
(12) Schoumacher, M.; Burbridge, M. Key roles of AXL and MER receptor tyrosine kinases in resistance to multiple anticancer therapies. *Curr. Oncol. Rep.* **2017**, *19*, 19.
(13) Gajiwala, K. S.; Grodsky, N.; Bolanos, B.; Feng, J.; Ferre, R.; Timofeevski, S.; Xu, M.; Murray, B. W.; Johnson, T. W.; Stewart, A. The Axl kinase domain in complex with a macrocyclic inhibitor offers first structural insights into an active TAM receptor kinase. *J. Biol. Chem.* **2017**, *292*, 15705−15716.
(14) Liu, J.; Yang, C.; Simpson, C.; DeRyckere, D.; Van Deusen, A.; Miley, M. J.; Kireev, D.; Norris-Drouin, J.; Sather, S.; Hunter, D.; Korboukh, V. K.; Patel, H. S.; Janzen, W. P.; Machius, M.; Johnson, G. L.; Earp, H. S.; Graham, D. K.; Frye, S. V.; Wang, X. Discovery of small molecule mer kinase inhibitors for the treatment of pediatric acute lymphoblastic leukemia. *ACS Med. Chem. Lett.* **2012**, *3*, 129−134.
(15) Huang, X.; Finerty, P., Jr.; Walker, J. R.; Butler-Cole, C.; Vedadi, M.; Schapira, M.; Parker, S.; Turk, B.; Thompson, D. A.; Dhe-Paganon, S. Structural insights into the inhibited states of the Mer receptor tyrosine kinase. *J. Struct. Biol.* **2009**, *165*, 88−96.
(16) Sheridan, C. First Axl inhibitor enters clinical trials. *Nat. Biotechnol.* **2013**, *31*, 775−776.
(17) Drexler, H. G.; Meyer, C.; Quentmeier, H. Effects of FLT3 ligand on proliferation and survival of myeloid leukemia cells. *Leuk. Lymphoma* **1999**, *33*, 83−91.
(18) Vardiman, J. W.; Thiele, J.; Arber, D. A.; Brunning, R. D.; Borowitz, M. J.; Porwit, A.; Harris, N. L.; Le Beau, M. M.; Hellstrom-Lindberg, E.; Tefferi, A.; Bloomfield, C. D. The 2008 revision of the World Health Organization (WHO) classification of myeloid neoplasms and acute leukemia: rationale and important changes. *Blood* **2009**, *114*, 937−51.
(19) Zeng, Q.; Cheng, Y.; Zhu, Q.; Yu, Z.; Wu, X.; Huang, K.; Zhou, M.; Han, S.; Zhang, Q. The relationship between overexpression of glial cell-derived neurotrophic factor and its RET receptor with progression and prognosis of human pancreatic cancer. *J. Int. Med. Res.* **2008**, *36*, 656−664.
(20) Morandi, A.; Martin, L. A.; Gao, Q.; Pancholi, S.; Mackay, A.; Robertson, D.; Zvelebil, M.; Dowsett, M.; Plaza-Menacho, I.; Isacke, C. M. GDNF-RET signaling in ER-positive breast cancers is a key determinant of response and resistance to aromatase inhibitors. *Cancer Res.* **2013**, *73*, 3783−3795.
(21) Gattei, V.; Degan, M.; Aldinucci, D.; De Iuliis, A.; Rossi, F. M.; Mazzocco, F. T.; Rupolo, M.; Zagonel, V.; Pinto, A. Differential expression of the RET gene in human acute myeloid leukemia. *Ann. Hematol.* **1998**, *77*, 207−210.
(22) Janning, M.; Ben-Batalla, I.; Loges, S. Axl inhibition: a potential road to a novel acute myeloid leukemia therapy? *Expert Rev. Hematol.* **2015**, *8*, 135−138.
(23) NCT02488408. *ClinicalTrials.gov*; U.S. National Institutes of Health: Bethesda, MD, 2015; www.clinicaltrials.gov (accessed Oct 19, 2017).
(24) Cetkovic-Cvrlje, M.; Uckun, F. M. Targeting Janus kinase 3 in the treatment of leukemia and inflammatory diseases. *Arch. Immunol. Ther. Exp.* **2004**, *52*, 69−82.
(25) Reiter, K.; Polzer, H.; Krupka, C.; Maiser, A.; Vick, B.; Rothenberg-Thurley, M.; Metzeler, K. H.; Dörfel, D.; Salih, H. R.; Jung, G.; Nößner, E.; Jeremias, I.; Hiddemann, W.; Leonhardt, H.; Spiekermann, K.; Subklewe, M.; Greif, P. A. Tyrosine kinase inhibition increases the cell surface localization of FLT3-ITD and enhances FLT3-directed immunotherapy of acute myeloid leukemia. *Leukemia* **2018**, *32*, 313−322.

DOI: 10.1021/acs.jmedchem.7b01605
J. Med. Chem. 2018, 61, 2104−2110